

Assessment of Waldeyer's ring in pediatric and adolescent Hodgkin lymphoma patients—Importance of multimodality imaging: Results from the EuroNet-PHL-C1 trial

Lars Kurch^{1,#}  | Christine Mauz-Körholz^{2,3,#} | Alexander Fosså⁴ |
 Thomas Walther Georgi¹ | Regine Kluge¹ | Jörg Martin Bartelt⁵ | Christian Kunze⁵ |
 Walter Alexander Wohlgemuth⁵ | Tanja Pelz⁶ | Dirk Vordermark⁶ | Sebastian Plößl⁷ |
 Dirk Hasenclever⁸ | Osama Sabri¹ | Judith Landman-Parker⁹ |
 William Hamish Wallace¹⁰ | Jonas Karlen¹¹ | Ana Fernández-Teijeiro¹² |
 Michaela Cepelova¹³  | Tomasz Klekawka¹⁴ | Ayca Muftuler Løndalen¹⁵ |
 Dagmar Steiner¹⁶ | Gabriele Krombach¹⁷ | Andishe Attarbaschi¹⁸  |
 Martha Hoffmann¹⁹ | Francesco Ceppi²⁰ | Jane Pears²¹ | Andrea Hraskova²² |
 Anne Uyttebroeck²³ | Auke Beishuizen^{24,25} | Karin Dieckmann²⁶ | Thierry Leblanc²⁷ |
 Stephen Daw²⁸ | Dieter Körholz² | Dietrich Stoevesandt⁵

¹ Department of Nuclear Medicine, University of Leipzig, Leipzig, Germany

² Department of Pediatric Hematology and Oncology, Justus-Liebig University, Gießen, Germany

³ Medical Faculty of the Martin-Luther-University, Halle (Saale), Germany

⁴ Department of Medical Oncology and Radiotherapy, Oslo University Hospital, Oslo, Norway

⁵ Department of Radiology, Medical Faculty of the Martin-Luther-University, Halle (Saale), Germany

⁶ Department of Radiation Oncology, Medical Faculty of the Martin-Luther-University, Halle (Saale), Germany

⁷ Department of Ear, Nose and Throat Medicine, Hospital Martha-Maria Halle, Halle (Saale), Germany

⁸ Institute for Medical Informatics, Statistics and Epidemiology (IMISE), University of Leipzig, Leipzig, Germany

⁹ Hôpital Armand-Trousseau Sorbonne Université, Paris, France

¹⁰ Department of Paediatric Oncology, Royal Hospital for Sick Children, University of Edinburgh, Edinburgh, UK

¹¹ Karolinska University Hospital, Astrid Lindgrens Childrens Hospital, Stockholm, Sweden

¹² Pediatric Onco-Hematology Unit, Hospital Universitario Virgen Macarena, Sevilla, Spain

¹³ Department of Pediatric Hematology and Oncology, University Hospital Motol and, Second Medical Faculty of Charles University, Prague, Czech Republic

¹⁴ Institute of Pediatrics, Jagiellonian University Medical College, Krakow, Poland

¹⁵ Department of Radiology and Nuclear Medicine, Oslo University Hospital, Oslo, Norway

¹⁶ Department of Nuclear Medicine, Justus-Liebig University Giessen, Giessen, Germany

¹⁷ Department of Radiology, Justus-Liebig University Giessen, Giessen, Germany

¹⁸ Department of Pediatric Hematology and Oncology, St. Anna Children's Hospital, Medical University of Vienna, Vienna, Austria

¹⁹ Wiener Privatklinik, Radiology Centre, Vienna, Austria

Abbreviations: ¹⁸F-FDG-PET, ¹⁸F-fluorodeoxyglucose positron emission tomography; ceCT, contrast-enhanced CT; CT, computed tomography; ENT, ear-nose-throat; EuroNet-PHL, European Network for Pediatric Hodgkin Lymphoma; EuroNet-PHL-C1, European Network for Pediatric Hodgkin Lymphoma, Classical Hodgkin Lymphoma, 1st trial generation; HL, Hodgkin lymphoma; IFRT, involved-field radiotherapy; MRI, magnetic resonance imaging; OEPA, vincristine, etoposide, prednisone, doxorubicin; PHL, pediatric Hodgkin lymphoma; WR, Waldeyer's ring.

This is an open access article under the terms of the [Creative Commons Attribution-NonCommercial-NoDerivs](https://creativecommons.org/licenses/by-nc-nd/4.0/) License, which permits use and distribution in any medium, provided the original work is properly cited, the use is non-commercial and no modifications or adaptations are made.

© 2021 The Authors. *Pediatric Blood & Cancer* published by Wiley Periodicals LLC

²⁰ Division of Pediatrics, Department of Woman-, Mother-Child, Pediatric Hematology-Oncology Unit, University Hospital of Lausanne, Lausanne, Switzerland

²¹ Department of Pediatric Hematology and Oncology, Our Lady's Children's Hospital, Dublin, Ireland

²² Department of Pediatric Hematology and Oncology, University Children's Hospital, Bratislava, Slovakia

²³ Department of Pediatric Hematology and Oncology, University Hospitals Leuven, Leuven, Belgium

²⁴ Erasmus MC-Sophia Children's Hospital, Rotterdam, The Netherlands

²⁵ Princess Máxima Center for Pediatric Oncology, Utrecht, The Netherlands

²⁶ Department of Radiation Oncology, University Hospital Vienna, Vienna, Austria

²⁷ Service d'Hématologie Pédiatrique, Hôpital Robert-Debré, Paris, France

²⁸ Department of Pediatric Hematology and Oncology, University College London Hospitals, London, UK

Correspondence

Dr. med. L. Kurch, Department of Nuclear Medicine, University Hospital of Leipzig, Liebigstraße 18, 04103 Leipzig, Germany.
Email: lars.kurch@medizin.uni-leipzig.de

#These authors contributed equally to this work

Abstract

Background: In the EuroNet Pediatric Hodgkin Lymphoma (EuroNet-PHL) trials, decision on Waldeyer's ring (WR) involvement is usually based on clinical assessment, that is, physical examination and/or nasopharyngoscopy. However, clinical assessment only evaluates mucosal surface and is prone to interobserver variability. Modern cross-sectional imaging technology may provide valuable information beyond mucosal surface, which may lead to a more accurate WR staging.

Patients, materials, and methods: The EuroNet-PHL-C1 trial recruited 2102 patients, of which 1752 underwent central review including reference reading of their cross-sectional imaging data. In 14 of 1752 patients, WR was considered involved according to clinical assessment. In these 14 patients, the WR was re-assessed by applying an imaging-based algorithm considering information from ¹⁸F-fluorodeoxyglucose positron emission tomography, contrast-enhanced computed tomography, and/or magnetic resonance imaging. For verification purposes, the imaging-based algorithm was applied to 100 consecutive patients whose WR was inconspicuous on clinical assessment.

Results: The imaging-based algorithm confirmed WR involvement only in four of the 14 patients. Of the remaining 10 patients, four had retropharyngeal lymph node involvement and six an inconspicuous WR. Applying the imaging-based algorithm to 100 consecutive patients with physiological appearance of their WR on clinical assessment, absence of WR involvement could be confirmed in 99. However, suspicion of WR involvement was raised in one patient.

Conclusions: The imaging-based algorithm was feasible and easily applicable at initial staging of young patients with Hodgkin lymphoma. It increased the accuracy of WR staging, which may contribute to a more individualized treatment in the future.

KEYWORDS

¹⁸F-FDG-PET, ENT investigation, MRI, multimodality imaging, CT, pediatric Hodgkin lymphoma, staging, Waldeyer's ring

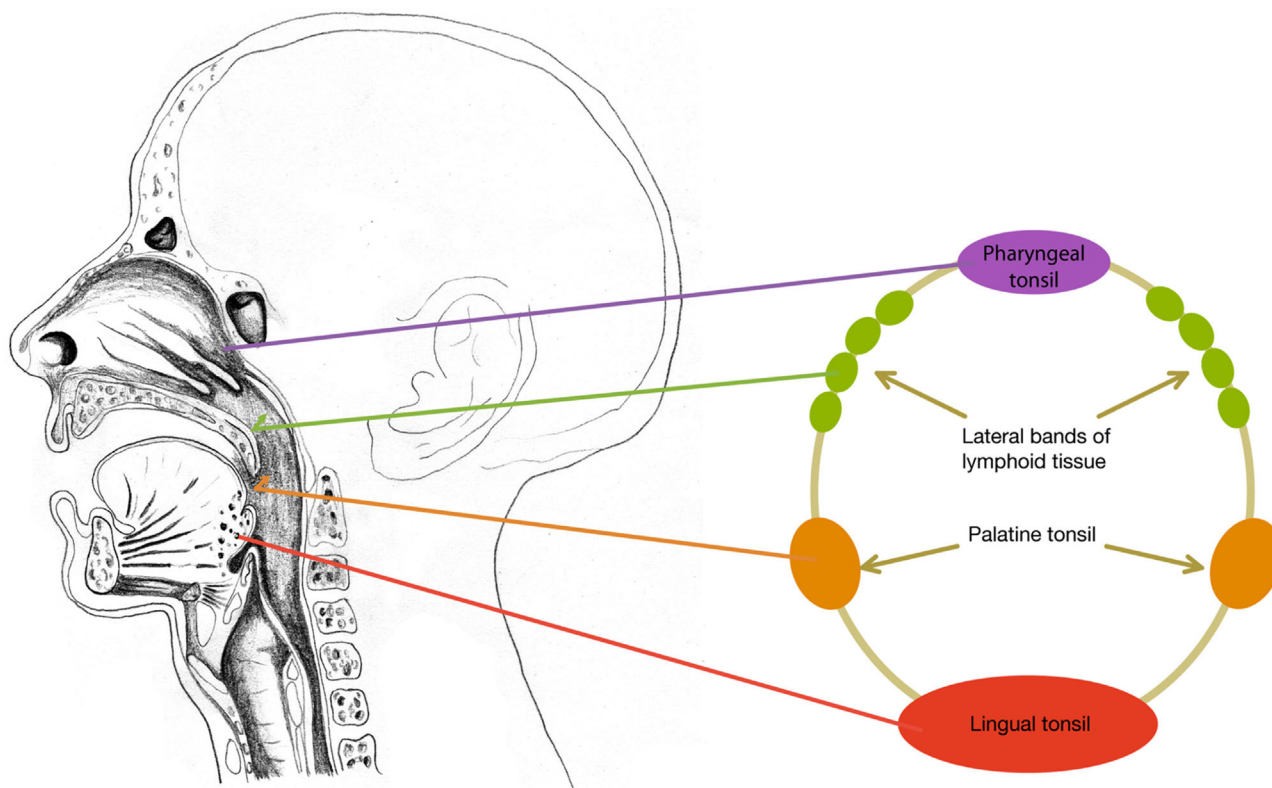


FIGURE 1 Anatomy of the Waldeyer's ring. Illustrated by C. Mannewitz, Leipzig, Germany

1 | BACKGROUND

Pediatric Hodgkin lymphoma (PHL) is highly curable by combined modality treatment consisting of chemotherapy and radiotherapy. However, radiotherapy is in particular responsible for treatment-related late effects.^{1,2} Trials on PHL aim at individualized, risk-adapted treatment to maintain high cure rates and to reduce late effects. The worldwide largest trials in young Hodgkin lymphoma (HL) patients were initiated by the North American Children's Oncology Group and the European Pediatric Hodgkin Lymphoma Group.^{3,4} Both groups work closely together to reach harmonization in staging and response assessment.⁵

The Waldeyer's ring (WR) is an independent lymphatic region and rarely involved in HL.^{6,7} An illustration of the WR anatomy is shown in Figure 1. In the original Ann Arbor classification, introduced at a time where imaging modalities were limited and therapy relied to a large part on now outdated radiotherapy techniques, the WR also included adjacent lymph nodes of the para- and retropharyngeal space.

In the North American Children's Oncology Group HL trials, the staging procedure of WR is not defined. In the European Network for Pediatric Hodgkin Lymphoma (EuroNet-PHL) trials, WR staging is usually performed by clinical assessment, that is, physical examination and/or nasopharyngoscopy.⁵

Clinical assessment obviously only assesses the appearance of the mucosal surface and possibly a displacement of the WR but not the

three-dimensional involvement of deeper adjacent structures. Furthermore, clinical findings used to conclude WR involvement are not specific which makes clinical assessment prone to high interobserver variability.^{8,9} Still, prior to the introduction of modern imaging technologies, clinical assessment was considered the staging method of choice to evaluate the entire WR.¹⁰ However, cross-sectional imaging technologies have improved much during the last 30 years and computed tomography (CT), magnetic resonance imaging (MRI), and ¹⁸F-fluorodeoxyglucose positron emission tomography (¹⁸F-FDG-PET) are widely available nowadays. Thus, it seems reasonable to include these modalities into the staging procedure and to assess their performance for a more adequate assessment of WR involvement.⁹

Adequate WR staging is especially important when radiotherapy is employed in the treatment protocol, that is, involved field radiotherapy (IFRT). Since the WR covers a large area of the hypo-, oro-, and nasopharynx, IFRT may consecutively lead to a large irradiation field.^{11,12}

The aim of this study was to evaluate the potential of morphological and metabolic cross-sectional imaging data for improving WR assessment.

2 | PATIENTS, MATERIALS, AND METHODS

Patient and imaging data analyzed in the present study are derived from the EuroNet-PHL-C1 trial (EudraCT: 2006-000995-33;

Clinicaltrial.gov: NCT00433459). This trial was initiated by the European Network for Pediatric Hodgkin Lymphoma (EuroNet-PHL). It recruited 2102 PHL patients (Classical HL) between 2007 and 2013.

1752 of the 2102 trial patients underwent the entire central review process including reference evaluation of their original cross-sectional imaging data in a standardized and structured manner.⁴ For initial staging and early response assessment, ¹⁸F-FDG-PET and contrast-enhanced CT (ceCT) from the upper neck to the upper thighs or, as an alternative, MRI of neck, abdomen, and pelvis as well as ceCT of the thorax were recommended. Data from all scans were stored on a highly secured server with all necessary software for image analyses provided.¹³

In central review, all lymphatic regions were assessed by cross-sectional imaging including volumetric measurements at initial staging and restaging. Since WR involvement was considered a “non-measurable” lymphatic region, WR evaluation at staging and restaging was usually based on clinical assessment, performed by the local pediatric oncologist or – preferentially – by an ear-nose-throat (ENT) specialist. No criteria were prespecified in the protocol for WR involvement and biopsy was not required. The results of clinical assessment were reported by the local department to the EuroNet study office and documented by central data management, respectively.

Independent of stage, all patients received two cycles of OEPA (vincristine, etoposide, prednisone, doxorubicin) induction chemotherapy.³ Patients with intermediate and high risk received two or four additional cycles, respectively, being randomly assigned to either COPP (cyclophosphamide, vincristine, procarbazine, prednisone) or COPDAC (cyclophosphamide, vincristine, prednisone, dacarbazine).³ IFRT to all initially involved sites (except for bone marrow lesions) was given to patients with ¹⁸F-FDG-PET positive disease after two courses of OEPA.³ ¹⁸F-FDG-PET positivity was defined according to the criteria released by the International Harmonization Project in Lymphoma.¹⁴

According to national legislation, the EuroNet-PHL-C1 trial was approved by ethics committees, medical agencies, and institutional review boards of the participating countries and centers. All patients and/or their guardians gave written informed consent. The institutional review board of the EuroNet-PHL-C1 trial approved this retrospective imaging data analysis and waived the requirement for additional informed consent.

The study presented here consists of three parts and described in detail as follows:

- (1) Construction of an imaging-based algorithm to systematically evaluate the WR

The imaging-based algorithm was created on the basis of specialized knowledge gained through more than 10 years of cross-sectional imaging data reference reading in PHL (LK and DiS), and evidence from the literature.^{8,9,15,16,17,18,19}

The imaging-based algorithm included four steps:

First, ¹⁸F-FDG-PET at staging was used as a screening tool. The components of the WR were checked visually for aspects of asymmetry, for example, side differences in the configuration and/or differences in the

¹⁸F-FDG uptake characteristics of the pharyngeal and/or palatine tonsils. According to a systematic review by Guimaraes et al, asymmetry was the most frequent sign of tonsillar lymphoma involvement.⁸ Completing this step, the WR was assigned to either category “symmetric” or “asymmetric.”

Second, the WR was evaluated morphologically on ceCT and/or MR images, either confirming or rebutting the assignment based on ¹⁸F-FDG-PET. If asymmetry was confirmed, ceCT and/or MR images were checked for alternative explanations beyond WR involvement.

Third, based on the results of steps (i) and (ii), the WR was categorized to be either involved (asymmetric WR on ¹⁸F-FDG-PET and confirmation of WR involvement on ceCT and/or MRI) or not involved (missing asymmetry on ¹⁸F-FDG-PET or asymmetry on ¹⁸F-FDG-PET but alternative morphological explanation for asymmetry).

For the fourth step, both metabolic and morphologic responses after two courses of OEPA were compared for both the WR area and the largest cervical lymphoma manifestation. Using the cervical lymphoma manifestation as a reference, cases were categorized based on the response of WR structures as having either a lymphoma-like response or a no-lymphoma-like response. Lymphoma-like response was only concluded if metabolic and morphologic responses of the WR area were similar to metabolic as well as morphologic response of the largest cervical lymphoma manifestation. Otherwise, a no-lymphoma-like response was determined, potentially attributable to upper respiratory tract infection or inflammation. The latter two are frequently found in young patients both before and during HL treatment.⁹

- (2) Application of the imaging-based algorithm to patients with WR involvement according to clinical assessment

Patients considered for this analysis met the following criteria:

- (i) Enrollment in the EuroNet-PHL-C1 trial.
- (ii) WR involvement was detected by clinical assessment.
- (iii) Central review including the original cross-sectional imaging data was performed.
- (iv) Cross-sectional imaging data were still available on the central study server.
- (v) Quality of cross-sectional imaging allowed sufficient re-evaluation.

- (3) Application of the imaging-based algorithm to patients without WR involvement according to clinical assessment

Each patient of the EuroNet-PHL-C1 trial was registered with a unique study identification number. Numbering either started with 2000 and ended at 3799 or started with 5000 and ended at 5400 (patients from Great Britain), respectively. The imaging-based algorithm was applied to 100 consecutive patients starting at study identification number 2001. They had to fulfill the following criteria:

TABLE 1 Characteristics of patients in whom WR involvement was determined by clinical assessment

Age	Mean, Range	11 years, 3–16 years
Sex	Female, Male	n = 6, n = 8
Histology	Mixed cellularity, Nodular sclerosis, No information	n = 7, n = 6, n = 1
Ann Arbor stage	IIA, IIB, IIIA, IIIB, IIIAE, IVAE, IVBE	n = 6, n = 1, n = 2, n = 2, n = 1, n = 1, n = 1

- (i) Enrollment in the EuroNet-PHL-C1 trial.
- (ii) WR was assessed as uninvolved by clinical assessment.
- (iii) Central review including the original cross-sectional imaging data was performed.
- (iv) Lymphoma lesions were detectable on at least one side of the upper neck (i.e., lymph node levels I–III and V).²⁰
- (v) Cross-sectional imaging data were still available on the central study server.
- (vi) Quality of cross-sectional imaging data allowed sufficient re-evaluation.

Relevant patient information (age, sex, histology, stage, early response in ¹⁸F-FDG-PET response) for parts (2) and (3) of this study was retrieved from the central database of the EuroNet-PHL-C1 study.

3 | RESULTS

(1) Patients with WR involvement according to clinical assessment

(a) Patient selection and characterization

Twenty-eight of 2102 (1.3%) EuroNet-PHL-C1 trial patients had documented involvement of the WR. Seventeen of 28 patients underwent central review including their cross-sectional imaging data. In 14 of the 17 patients, WR involvement was determined by clinical assessment. Characteristics of these 14 patients are shown in Table 1.

In three of the 17 patients, WR involvement was determined only by cross-sectional imaging data, whereas clinical assessment was either not performed or negative. These patients were excluded from analyses. However, detailed case descriptions are provided in the supplement.

Figure 2 displays stepwise patient selection.

(b) Structured image analysis

Figure 3 shows the results after applying the imaging-based algorithm to the 14 EuroNet-PHL-C1 patients assigned to have WR involvement according to clinical assessment.

In eight of 14 patients, the WR showed asymmetric aspects on ¹⁸F-FDG-PET, which were confirmed by ceCT and/or MRI.

In four of these eight patients, asymmetry was due to a well-delimitable retropharyngeal lymph node adjacent to the WR (Figure 4). Following two cycles of OEPA, these lymph nodes had either disappeared or markedly shrunken in size and metabolism had markedly decreased, consistent with a lymphoma-like response.

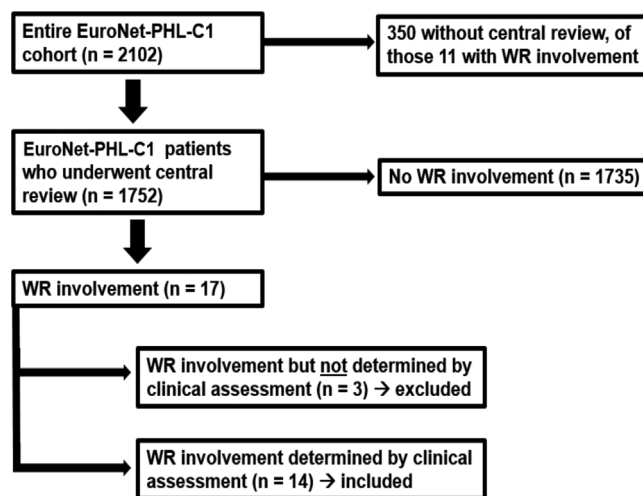


FIGURE 2 Consort flow chart: Selection of patients who were determined to have WR involvement according to clinical assessment and who underwent central review

In the other four patients, asymmetry on ¹⁸F-FDG-PET images could not be explained by anything else than through WR involvement (Figure 5). The metabolically active mass was located in one of the anatomic components of the WR and other reasons for asymmetry could be excluded by ceCT and/or MRI. After induction chemotherapy, asymmetry disappeared completely (Figure 5). Comparing both metabolic and morphological responses of the involved WR area with the corresponding responses of the largest cervical lymphoma lesion resulted in a lymphoma-like response in all four cases.

In six of 14 patients the WR showed a symmetric pattern without any sign of lymphoma, neither on ¹⁸F-FDG-PET nor on ceCT and/or MR images. In five of these six patients, the WRs responded morphologically and metabolically differently compared to the largest cervical lymphoma lesion, consistent with a no-lymphoma-like response. Together with the symmetric pattern at staging, the absence of a lymphoma-like response made WR involvement unlikely. However, in one patient the response of the WR to induction chemotherapy was similar to the response of the largest cervical lymphoma lesion, resulting in a lymphoma-like response according to our definition. In this case, the unlikely diagnosis of a diffuse, superficial infiltration by HL could not be ruled out completely by image analysis.

In summary, the applied imaging-based algorithm confirmed WR involvement in only four of the 14 cases. In the majority of cases, however, the imaging-based algorithm led to a different conclusion compared to the clinical assessment. In concrete terms, retropharyngeal lymph node involvement was diagnosed in four cases instead

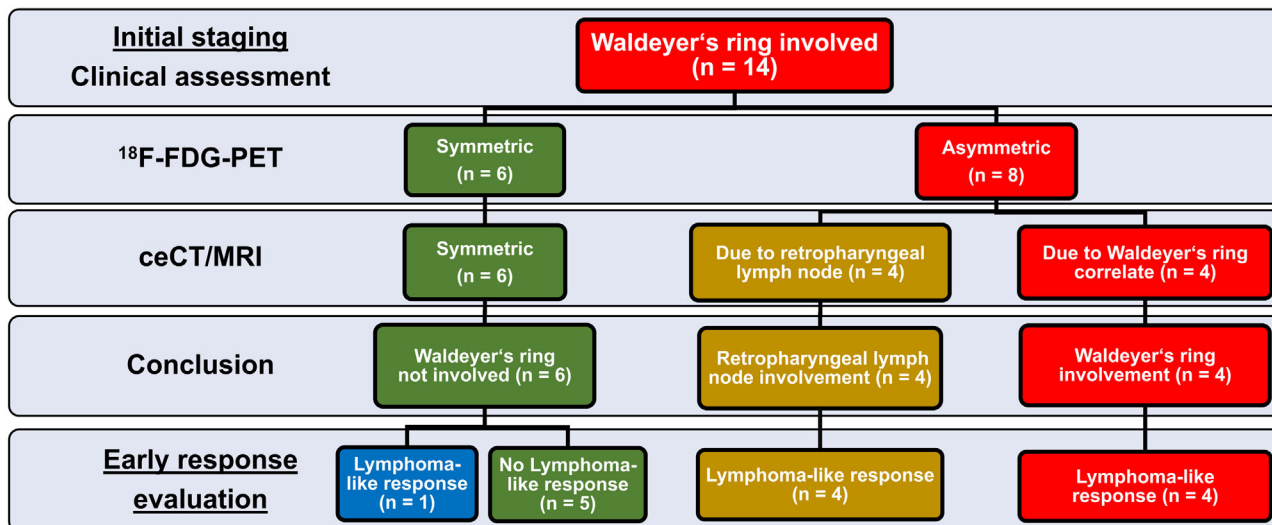


FIGURE 3 Flow chart with results from image analysis of patients with WR involvement according to clinical assessment

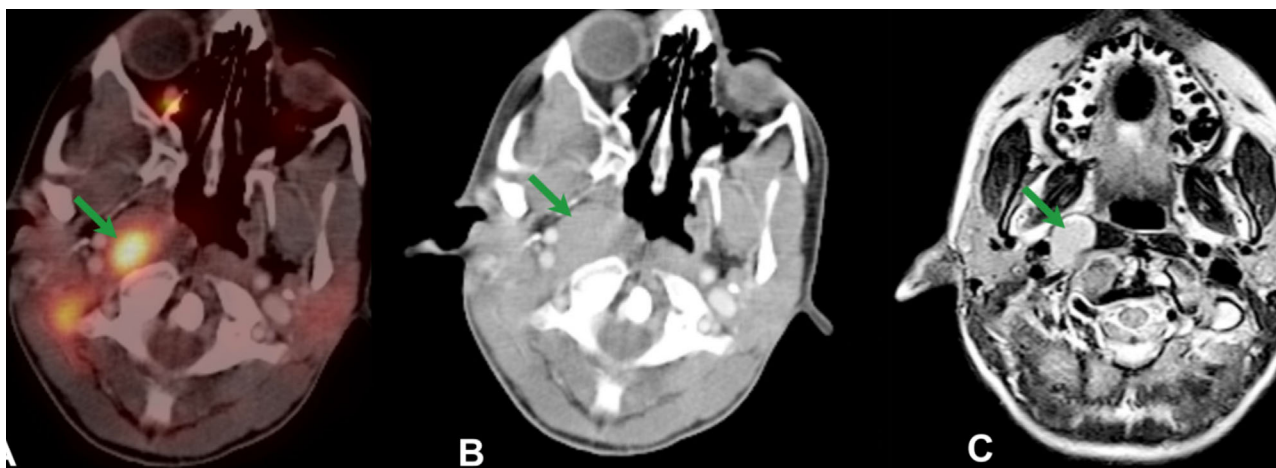


FIGURE 4 Patient with asymmetric Waldeyer's ring on ¹⁸F-FDG-PET imaging (A) explainable on CT and MR images by a retropharyngeal lymph node directly adjacent to the right palatine tonsil (B and C)

of WR involvement, and in five cases there was no evidence of either WR or retropharyngeal lymph node involvement. Only one case remained somewhat unclear due to its lymphoma-like response to chemotherapy.

(2) Structured image analysis in patients without WR involvement on clinical assessment

The structured image analysis was applied to 100 consecutive patients without any sign of WR involvement according to clinical assessment. Respective patient data are shown in Table 2, and results of the structured image analysis are shown in Figure 6.

17 of the 100 consecutive patients showed asymmetric ¹⁸F-FDG uptake pattern of their WR. In 14 of 17 patients, asymmetry could also be confirmed on ce/CT and/or MRI. However, 13 had reasonable

explanations beyond HL involvement of the WR, like retropharyngeal lymph nodes (n = 9), concomitant ENT infections, for example, by signs of sinusitis (n = 3), or displacement of WR components by an airway device (n = 1). Only in one patient a morphological correlate within the pharyngeal tonsil was detectable which appeared irregular, was difficult to delineate, and had a very strong contrast enhancement in ceCT. These features made the lesion highly suspicious of WR involvement. In five of 14 patients, the WR or the lesions responsible for asymmetry showed a lymphoma-like response (4× retropharyngeal lymph node, 1× suspicion of WR involvement), whereas no-lymphoma-like response was determined in nine of 14 patients (5× retropharyngeal lymph nodes, 3× ENT infection, 1× airway device).

Three of 17 patients with asymmetric appearance of the WR on ¹⁸F-FDG had no morphologic correlate neither in the WR nor in adjacent structures and showed a no-lymphoma-like response. Thus,

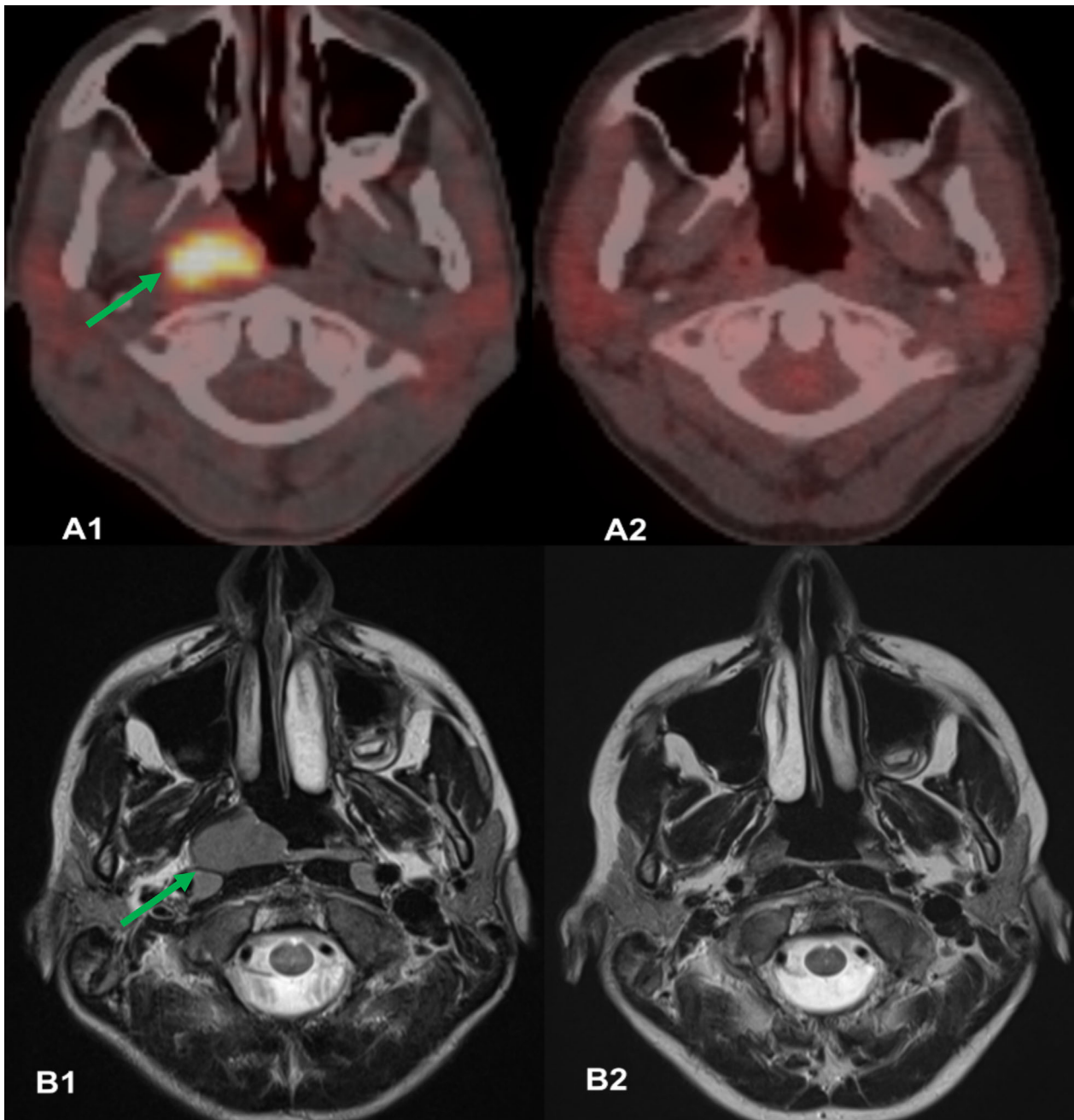


FIGURE 5 Combined low-dose ^{18}F -FDG-PET/CT images (A1, A2) and MR images (B1, B2) show Waldeyer's ring involvement at initial staging (A1, B1) and normalization following two courses of OEPA chemotherapy (A2, B2)

TABLE 2 Characteristics of patients in whom WR involvement was excluded by clinical assessment

Age	Mean, Range	11.8 years, 3-17 years
Sex	Female, Male	n = 37, n = 63
Histology	Mixed cellularity, Nodular sclerosis, Lymphocyte rich, No information	n = 28, n = 56, n = 4, n = 12
Ann Arbor stage	IA, IIA, IIB, IIBE, IIIA, IIIB, IVA, IVB, IVBE	n = 4, n = 42, n = 9, n = 5, n = 9, n = 9, n = 7, n = 11, n = 4

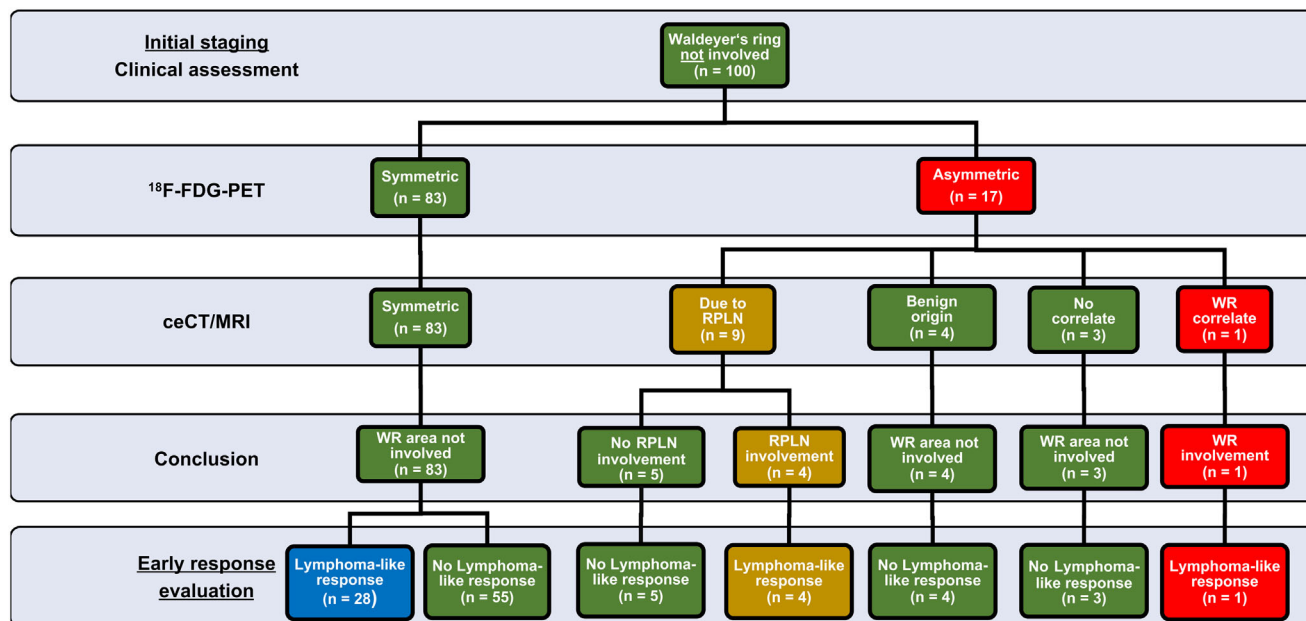


FIGURE 6 Flow chart of the imaging-based algorithm applied to 100 patients without Waldeyer's ring involvement according to clinical assessment. WR, Waldeyer's ring; RPLN, retropharyngeal lymph node

non-specific benign disorders like lymphoid hyperplasia were most likely.

83 of the 100 patients showed a symmetric and homogeneous uptake of their WR on ^{18}F -FDG-PET images. Correspondingly, neither ceCT nor MRI showed any structural abnormalities. 28 of these 83 patients had a lymphoma-like response, whereas 55 showed a no-lymphoma-like response.

4 | DISCUSSION

About 1% of the patients enrolled into the EuroNet-PHL-C1 trial had WR involvement which is compatible with other reports showing that the WR is rarely involved by Hodgkin's lymphoma.^{8,9} Nevertheless, precise staging of the WR including the differentiation between directly adjacent lymph nodes and the WR is crucial when radiotherapy is a component of the treatment. Currently, assessment of the WR at staging in HL patients is commonly performed by clinical assessment, sometimes involving a detailed examination by an ENT specialist. However, especially in the absence of biopsies, clinical assessment remains highly subjective, and is therefore not recommendable as the sole method of diagnosis.⁹

Therefore, an imaging-based algorithm was developed and retrospectively tested on two different cohorts of PHL patients treated in the EuroNet-PHL-C1 trial. Building on the study results of Guimaraes et al, symmetric versus asymmetric appearance of the WR was chosen as the key criterion to decide on WR involvement and non-involvement, respectively. From a pathophysiological perspective, morphological changes in tissues follow metabolic changes. Based on this principle, ^{18}F -FDG-PET images were used to sensitively screen for any signs of asymmetry. However, in children and adolescents there is a

variety of non-malignant conditions, which may lead to either a homogeneously elevated or an asymmetric glucose uptake.^{9,10,17,19} In order to gain specificity, ^{18}F -FDG-PET results were further assessed by ceCT and/or MRI. In addition, the WR and adjacent structures were compared to chemotherapy response in nodal cervical HL lesions.

For the patients whose WR was evaluated as involved by clinical assessment and who underwent central review ($n = 14$), we were able to demonstrate that a structured analysis of modern imaging substantially contributed to a more precise WR staging. Most strikingly, in 29% of these patients ($n = 4$), WR involvement was confirmed. In another 29%, clinical suspicion of WR involvement was well explainable by involved retropharyngeal lymph nodes adjacent to the WR ($n = 4$). Retropharyngeal lymph nodes occur in over 90% of all children and can be a plausible reason for asymmetry.^{9,16} However, most retropharyngeal lymph nodes are of benign origin.^{9,16} To differentiate best between retropharyngeal lymph nodes and lymphatic tissue of the WR, MRI is preferable over ceCT because of a higher soft tissue contrast. The remaining more than 40% ($n = 6$) had an entirely inconspicuous appearance of the WR in both ^{18}F -FDG-PET and ce/CT or MRI. This may be due to the fact that mucous membrane alterations as evaluated by clinical assessment are unspecific signs of a possible involvement, especially when diagnosed because of color alterations or mucosal lesions.⁸ In this respect, one could argue that superficial and diffuse lymphoma infiltrations are not detectable on cross-sectional imaging and that diffuse infiltrations may lead to an increased, yet homogenous and symmetric glucose metabolism on ^{18}F -FDG-PET images. Since asymmetry in ^{18}F -FDG uptake was a key criterion to prompt further structured analysis, such cases could be missed. However, as frequently published, for example, for skeletal involvement, HL lesions are regularly of focal and not diffuse appearance in ^{18}F -FDG-PET.^{21,22} Furthermore, five of these six patients did not show ^{18}F -FDG-PET response

compatible with lymphoma manifestation when reanalyzed after two cycles of chemotherapy. Thus, in only one patient the absolutely rare constellation of a diffuse, superficial infiltration by HL could not be ruled out completely by image analysis.

The proposed imaging-based algorithm was also tested for 100 patients who were negative for WR involvement on clinical assessment. Seventeen of these 100 patients showed asymmetric patterns of their WR region on ^{18}F -FDG-PET images. The main reason for asymmetry was a retropharyngeal lymph node ($n = 9$, 53%). Retropharyngeal lymph nodes are frequently found in children but are not necessarily involved by lymphoma.^{9,16} Based on our algorithm, retropharyngeal lymph nodes were most likely involved in four patients as these lymph nodes were ^{18}F -FDG-avid and morphologically enlarged at staging and showed a lymphoma-like response following two courses of chemotherapy. Other common reasons for asymmetry in this cohort were non-specific benign disorders, for example, acute and chronic ENT inflammation or lymphoid hyperplasia ($n = 6$, 35%). Guimaraes et al reported on tonsillar asymmetry in children and adolescents. According to their results tonsillar asymmetry was of non-specific origin in even 74% of the cases.¹⁷ Besides, it is also noteworthy that in children who need narcosis to get their images performed, structures of the WR can be displaced by airway devices as detected in one patient of our cohort. This might be a source of misinterpretation when imaging data are evaluated. Interestingly, in one of the 17 patients with asymmetric WR appearance but negative clinical WR assessment, WR involvement was concluded on the basis of morphological and metabolic images. This lesion also showed a lymphoma-like response following two courses of OEPA chemotherapy. 83 of 100 patients had a symmetric appearance of their WR area both on ^{18}F -FDG-PET and on ceCT and/or MRI. In this patient group, WR response following two courses of OEPA chemotherapy is of special interest: 28 of 83 patients (34%) showed a lymphoma-like response through neither clinical assessment nor imaging data raised suspicion of WR involvement. Thus, a lymphoma-like response is only informative in cases of clear suspicion of WR involvement or involved retropharyngeal lymph nodes at initial staging.

The analysis of the two cohorts shows that the imaging-based algorithm contributes to an accurate staging of the WR area. This is especially important in case of an indication for WR irradiation. The Ann Arbor staging system defines the WR as a coherent site. Thus, in many HL study protocols the WR is considered as one coherent site which is treated in its entirety even if only one subsite is involved. However, irradiation of the entire WR will affect many structures of the head and neck like salivary glands, the thyroid and brain-supplying blood vessels.²³ This increases the risk of sicca syndrome, thyroid cancer, hypothyroidism, or atherosclerosis in later life.¹⁷ Guidelines from the International Lymphoma Radiation Oncology Group (ILROG) consider each of the WR subsites as independent and recommend for aggressive non-HLs of the WR not to irradiate the entire WR after chemotherapy anymore.²⁴ However, in the setting of combined modality treatment, the optimal radiation volume for pediatric patients with HL remains uncertain. Nevertheless, precise delineation of both WR and adjacent lymph nodes before treatment is important for any rational reduction

in volumes especially when new irradiation technologies like proton therapy are applied.²⁵

Although this is a large and comprehensive analysis, there are limitations: WR involvement determined by clinical assessment was reassessed by a dedicated imaging-based algorithm. None of the cases confirmed by the imaging-based algorithm was confirmed by biopsy. However, the introduction of WR biopsy would be much too invasive and would delay treatment start. The added value of such a biopsy-proven approach would be very limited with respect to event-free and overall survival, given the extremely small rate of WR involvement.

In summary, our analysis shows that the imaging-based algorithm is at least as reliable as clinical assessment for detecting involvement of WR in HL. In addition to this, the imaging-based algorithm is more sensitive, as in the cohort of 100 consecutively chosen patients clinical assessment is considered to have no WR involvement, the algorithm detected one case with clear signs of WR involvement on imaging. Most importantly, the imaging-based algorithm is much more specific, as it can differentiate between involvement of the WR itself, involvement of retropharyngeal lymph nodes, and other not lymphoma-related reasons, which might lead to a misdiagnosis of WR involvement on clinical assessment. This has significant consequences for therapy, especially the extent of possible radiotherapy with its known potential long-term adverse effects. Additionally, the imaging—the algorithm is based on—is nowadays usually done routinely on initial staging, therefore replacing determination of WR involvement by clinical assessment at initial staging with the imaging-based algorithm will produce no extra costs but will even save time and effort of both pediatricians and ENT specialists as well as patients necessary for clinical assessment of the WR. Consequently, the imaging-based algorithm will replace clinical assessment for determination of WR involvement in future protocols of the EuroNet-PHL consortium.

CONFLICT OF INTEREST

The authors declare that there is no conflict of interest.

AUTHOR CONTRIBUTIONS

Conception and design: LK, CMK, TP, SP, JMB, DK, and DiS. Data acquisition: LK, CMK, AF, TWG, RK, CK, TP, DV, DH, JLP, WHW, JK, JMB, AFT, MC, TK, AML, DS, GAK, AA, MH, FC, JP, AH, AU, AB, TL, SD, DK, and DiS. Data analysis: LK, CMK, AF, TWG, JMB, TP, DV, DH, DK, and DiS. Data interpretation: LK, CMK, AF, TWG, RK, CK, WAW, JBM, TP, DV, SP, DH, OS, JLP, WHW, JK, AFT, MC, TK, AML, DS, GAK, AA, MH, CF, JP, AH, AU, AB, KD, TL, SD, DK, and DiS. Drafting: LK, CMK, TWG, RK, JMB, TP, DV, DK, and DiS. Visualization: LK, JBM, DS, GAK, DiS, and AML. Revising: LK, CMK, AF, TWG, RK, CK, WAW, JMB, TP, DV, SP, DH, OS, JLP, WHW, JK, AFT, MC, TK, AML, DS, GAK, AA, MH, FC, JP, AH, AU, AB, DK, TL, SD, DK, and DiS. Final approval and agreement to be accountable for all aspects of the work: LK, CMK, AF, TWG, RK, CK, WAW, JMB, TP, DV, SP, DH, OS, JLP, WHW, JK, AFT, MC, TK, AML, DS, GAK, AA, MH, FC, JP, AH, AU, AB, DK, TL, SD, DK, and DiS.

ACKNOWLEDGMENT

Open access funding enabled and organized by Projekt DEAL.

DATA AVAILABILITY STATEMENT

The data (tables) that support the findings of this study are available from the corresponding author upon reasonable request provided the EuroNet-PHL study consortium agrees to that.

ORCID

Lars Kurch  <https://orcid.org/0000-0002-3396-4880>

Michaela Cepelova  <https://orcid.org/0000-0001-7191-588X>

Andishe Attarbaschi  <https://orcid.org/0000-0002-9285-6898>

REFERENCES

- Bhatia S, Yasui Y, Robison LL, et al. High risk of subsequent neoplasms continues with extended follow-up of childhood Hodgkin's disease: report from the Late Effects Study Group. *J Clin Oncol*. 2003;21:4386-4394.
- Schellong G, Riepenhausen M, Bruch C, et al. Late valvular and other cardiac diseases after different doses of mediastinal radiotherapy for Hodgkin disease in children and adolescents: report from the longitudinal GPOH follow-up project of the German-Austrian DAL-HD studies. *Pediatr Blood Cancer*. 2010;55:1145-1152.
- Mauz-Körholz C, Metzger ML, Kelly KM, et al. Pediatric Hodgkin lymphoma. *JCO*. 2015;33:2975-2985.
- Kluge R, Kurch L, Georgi T, Metzger M. Current role of FDG-PET in pediatric Hodgkin's lymphoma. *Semin Nucl Med*. 2017;47:242-257.
- Flerlage JE, Kelly KM, Beishuizen A, et al. Staging Evaluation and Response Criteria Harmonization (SEARCH) for Childhood, Adolescent and Young Adult Hodgkin Lymphoma (CAYAHL): methodology statement. *Pediatr Blood Cancer*. 2017;64:e26421.
- Kaplan HS, Rosenberg SA. The treatment of Hodgkin's disease. *Med Clin North Am*. 1966;50:1591-1610.
- Karnofsky DA. The staging of Hodgkin's disease. *Cancer Res*. 1966;26:1090-1094.
- Guimaraes AC, de Carvalho GM, Bento LR, Correa C, Gusmoa RJ. Clinical manifestations in children with tonsillar lymphoma: a systematic review. *Crit Rev Oncol Hematol*. 2014;90:146-151.
- Seelisch J, de Alarcon P, Flerlage J, et al. Expert consensus statements for Waldeyer's ring involvement in pediatric Hodgkin lymphoma: the Staging, Evaluation, and Response Criteria Harmonization (SEARCH) for Childhood, Adolescent and Young Adult Hodgkin lymphoma (CAYAHL) Group. *Pediatr Blood Cancer*. 2020;16:e28361.
- Brodsky L. Modern assessment of tonsils and adenoids. *Pediatr Clin North Am*. 1989;36:1551-1569.
- Li Y-X, Fang H, Lui Q-F, et al. Clinical features and treatment outcome of nasal-type NK-T-cell lymphoma of Waldeyer ring. *Clin Trials Obs*. 2008;112:3057-3064.
- Qin Y, Lijuan Lu, Lu Y, Yang K. Hodgkin lymphoma involving the tonsil misdiagnosed as tonsillar carcinoma: a case report and review of the literature. *Medicine*. 2018;97:e976.
- Kurch L, Mauz-Körholz C, Bertling S, et al. The EuroNet paediatric Hodgkin network—modern imaging data management for real time central review in multicentre trials. *Klin Padiatr*. 2013;225:357-361.
- Juweid ME, Stroobants S, Hoekstra OS, et al. Use of positron emission tomography for response assessment of lymphoma: consensus of the Imaging Subcommittee of International Harmonization Project in Lymphoma. *JCO*. 2007;25(5):571-578.
- Akcaay A, Kara CO, Dagdeviren E, Zencir M. Variation in tonsil size in 4- to 17-year-old schoolchildren. *J Otolaryngol*. 2006;35:270-274.
- Costa NS, Salisbury SR, Donnelly LF. Retropharyngeal lymph nodes in children: a common imaging finding and potential source of misinterpretation. *AJR Am J Roentgenol*. 2011;196:433-437.
- Guimaraes AC, de Carvalho GM, Correa CRS, Gusmoa RJ. Association between unilateral tonsillar enlargement and lymphoma in children: a systematic review and meta-analysis. *Crit Rev Oncol Hematol*. 2015;93:304-311.
- Nemec SF, Krestan CR, Noebauer-Huhmann IM, et al. Radiological normal anatomy of the larynx and pharynx and imaging techniques. *Radiologe*. 2009;49:8-16.
- Shammas A, Lim R, Charron M. Pediatric FDG PET/CT: physiologic uptake, normal variants, and benign conditions. *Radiographics*. 2009;29:1467-1486.
- Som PM, Curtin HD, Mancuso AA. Imaging-based nodal classification for evaluation of neck metastatic adenopathy. *AJR*. 2000;174:837-844.
- Hassan A, Siddique M, Bashir H, et al. (18)F-FDG-PET-CT imaging versus bone marrow biopsy in pediatric Hodgkin's lymphoma: a quantitative assessment of marrow uptake and novel insights into clinical implication of bone marrow involvement. *Eur J Nucl Med Mol Imaging*. 2017;44:1198-1206.
- Purz S, Mauz-Körholz C, Körholz D, et al. 18F-Fluorodeoxyglucose positron emission tomography for detection of bone marrow involvement in children and adolescents with Hodgkin's lymphoma. *J Clin Oncol*. 2011;29:3523-3528.
- Bi X-W, Li Y-X, Fang H, et al. High-dose and extended-field intensity modulated radiation therapy for early stage NK/T-cell lymphoma of Waldeyer's ring: dosimetric analysis and clinical outcome. *Int J Radiat Oncol Biol Phys*. 2013;87:1086-1093.
- Yahalom J, Illidge T, Specht L, et al. Modern radiation therapy for extranodal lymphomas: field and dose guidelines from the International Lymphoma Radiation Oncology Group. *Int J Radiat Oncol Biol Phys*. 2015;92:11-31.
- Lautenschläger S, Iancu G, Flatten V, et al. Advantage of proton-radiotherapy for pediatric patients and adolescents with Hodgkin's disease. *Radiat Oncol*. 2019;14:157.

SUPPORTING INFORMATION

Additional supporting information may be found online in the Supporting Information section at the end of the article.

How to cite this article: Kurch L, Mauz-Körholz C Fosså A, et al. Assessment of Waldeyer's ring in pediatric and adolescent Hodgkin lymphoma patients—Importance of multimodality imaging: Results from the EuroNet-PHL-C1 trial. *Pediatr Blood Cancer*. 2021;68:e28903. <https://doi.org/10.1002/pbc.28903>